Hindawi

Research Article

Ni(II), Cu(II), Mn(II), and Fe(II) Metal Complexes Containing 1,3-Bis(diphenylphosphino)propane and Pyridine Derivative: Synthesis, Characterization, and Antimicrobial Activity

Maged S. Al-Fakeh [iD],[1,2] **Gadah A. Allazzam,**[1] **and Naeema H. Yarkandi**[3]

[1]*Chemistry Department, College of Science, Qassim University, Buraidah 51452, Saudi Arabia*
[2]*Taiz University, Taiz, Yemen*
[3]*Chemistry Department, Faculty of Applied Science, Umm Al-Qura University, Makkah, Saudi Arabia*

Correspondence should be addressed to Maged S. Al-Fakeh; alfakehmaged@yahoo.com

Four of the coordination compounds of the general formula, [M(DPPP)(APY)(H$_2$O) Cl$_2$].xH$_2$O, where M = Ni(II), Cu(II), Mn(II), and Fe(II) and x = 0, 1, or 2 molecules of H$_2$O, DPPP = 1,3-bis(diphenylphosphino)propane, and APY = 2-aminopyridine, have been prepared and characterized. The structure of the complexes has been confirmed by elemental analysis, FT-IR, and UV-Vis spectral data. Thermal analysis (thermogravimetry, derivative thermogravimetry, and differential thermal studies) has been used to study the thermal decomposition stages. Biological activity of all synthesized complexes was tested against five bacterial strains and three fungal strains. Bacteria and fungi strains are common contaminants of the environment in Saudi Arabia, some of which are frequently reported from contaminated water, soil, and food.

1. Introduction

Coordination compounds have been known since the beginning of modern chemistry; also, coordination compounds are so common that their structures and reactions are described as in many ways. The atom within a ligand is bonded to the central metal atom. Especially in hydrometallurgy, the coordination chemistry of the metals participate plays a large role in their solubility and reactivity, as the ore is refined into a precious transition elements. Diphosphine ligands, such as 1,3-bis(diphenylphosphino) propane, are organophosphorus compounds, and these compounds are white solids that are soluble in organic solvents. It is also degraded in air to phosphine oxide and slightly air-sensitive. It is classified as a diphosphine ligand in coordination chemistry and homogeneous catalysis [1–3]. The mixed use of metal complexes containing diphosphines and other ligands, which consist of N or S atoms have been intensively inspected during the past years because of their

possibility applications in the fields of light emitting devices, biological activity, and catalysis [4–8]. Additionally, a pronounced attention has been induced by the investigation of the new bioactivity of metal-organic framework materials (BIOMOFs) contained in construction materials as potential antifungal and antibacterial materials (e.g., antifungal glass, antibacterial coating, or antibacterial) [9–14]. Diphosphines are essential ligand backbones, which are coordinated to the metal via monodentate or bidentate manner, and these ligands were used in the development of biologically active metal coordination complexes [15–18]. Pyridine derivatives avail as useful chelating ligands in a large form of inorganic and organometallic applications, and additions act as monodentate ligands that coordinate transition metal ions (N–Ni, N–Cu, Mn–N, and Fe–N) occupy an important position in organometallic chemistry. In addition, there are several reports on pyridine derivative compounds in which the amino group (NH$_2$) also participates in coordination [19–23]. In view of the above importance of these ligands

and its complexes, we report in this work on the synthesis and characterization of Ni(II), Cu(II), Mn(II), and Fe(II) coordination compounds with DPPP and APY. The structures of the ligands are presented in Figure 1.

2. Experimental

2.1. Materials. High purity 1,3-bis(diphenylphosphino) propane and 2-aminopyridine were supplied from Sigma Aldrich grade. They were purchased and used without purification.

2.2. Physical Measurements. The chemical analyses, CHN, were performed using, Analyischer Functions test Var. El Fab Nr. (11982027) elemental analyzer. FT-IR were recorded as potassium bromide disks (400 to 4000 cm^{-1}) with a FT-IR spectrophotometer and the UV-Vis spectra were obtained using a Shimadzu (UV-2101) PC spectrophotometer. Magnetic susceptibility measurements were done on a magnetic susceptibility balance of the type (MSB-Auto). The conductance of the complexes was measured using a conductivity meter model (4310, JENWAY). Thermal analysis of the compounds was carried out in dynamic air on a Shimadzu (DTG 60-H) thermal analyzer at a heating rate (10°C min^{-1}).

2.3. Antimicrobial Activity of the Complexes

2.3.1. Bacterial and Fungal Strains. The antimicrobial activity of different four complexes extracts was evaluated using five bacterial strains and three fungal strains. Three strains of gram-positive cocci (*Staphylococcus epidermidis, Enterococcus faecalis,* and *Staphylococcus aureus*), two strains of gram-negative bacilli (*Escherichia coli,* and *Pseudomonas aeruginosa*), one stain of yeast-like fungi (*Candida albicans*), and 2 molds (*Aspergillus fumigatus* and *Aspergillus flavus*) were used in this study.

2.3.2. Inoculum Preparation. Bacterial and yeast-like fungal inoculum were prepared from fresh pure cultures in Muller Hinton broth. Each bacterial and yeast-like fungal suspension were compared with 0.5 McFarland standard. Mold samples were inoculated directly into Sabouraud dextrose agar.

2.3.3. Agar Diffusion Assay. The antimicrobial activity of different chemical complex extracts against the selected microorganisms was evaluated using the agar diffusion assay. Each bacterial inoculum was spread on to two Mueller–Hinton agar plates using a sterile cotton swab by lawn culture technique, and the mold samples were inoculated directly onto Sabouraud dextrose agar. After inoculation, wells were made with the help of a sterile cork borer; three wells were made in one of the agar plates for extract numbers 1–3, and four wells were made in the second plate for extract numbers 4–7. Then, each extract (100 μl) was added to already marked well. The plates were then incubated for 18–24 hrs at 37°C. After incubation, we observed the zone of inhibition around the wells and measured the zone diameter in millimeters (mm) by a ruler.

2.4. Preparation of the Four Complexes

2.4.1. Preparation of [Ni(DPPP)(APY)(H$_2$O)Cl$_2$].H$_2$O Complex (1). An aqueous solution (10 mL) of NiCl$_2$.6H$_2$O (0.46 g, 1.9 mmol) was added to 1,3-bis(diphenylphosphino) propane (DPPP) (0.8 g, 1.9 mmol) of CH$_2$Cl$_2$ in 10 mL in the presence of NaOH (0.1 M). To the whole solution, an ethanolic solution (10 mL) of 2-aminopyridine (APY) (0.18 g, 1.9 mmol) was added. Pale brown precipitate was separated after refluxing for 3 h. The precipitate was filtered out after being cooled, washed with distilled water and ethanol, and then dried over P$_2$O$_5$ in a dissector.

2.4.2. Preparation of [Cu(DPPP)(APY)(H$_2$O)Cl$_2$] Complex (2). The complex was synthesized by adding the CuCl$_2$.2H$_2$O solution (0.82 g, 4.8 mmol) in 20 mL distilled water to 2 g (4.8 mmol) of 1,3-bis(diphenylphosphino)propane in 10 mL of CH$_2$Cl$_2$ in the presence of NaOH (0.1 M). Then, to the mixture solution, a 15 mL ethanolic solution of APY (0.45 g, 4.8 mmol) was added immediately. The mixture was refluxed for 3 h and then left aside at room temperature. A light green color was produced and the latter was separated and washed with H$_2$O and ethanol.

2.4.3. Preparation of [Mn(DPPP)(APY)(H$_2$O)Cl$_2$] Complex (3). The Mn(II) complex was prepared by adding the metal salt MnCl$_2$.4H$_2$O (0.87 g, 4.4 mmol) dissolved in 20 mL of distilled water with DPPP ligand (1.8 g, 4.4 mmol) dissolved in about 15 mL of a solution (1:2 MeOH/CH$_2$Cl$_2$) in the presence of NaOH. The subsequent process was the addition of a 10 ml ethanolic solution of APY ligand (0.41 g, 4.4 mmol). The mixture was refluxed for about 4 h and then cooled. The dark-brown color formed separated, which was filtered and washed with EtOH and dried over P$_2$O$_5$.

2.4.4. Preparation of [Fe(DPPP)(APY)(H$_2$O)Cl$_2$].2H$_2$O Complex (4). A 1,3-bis(diphenylphosphino)propane (2 g, 4.8 mmol) was dissolved in 15 mL of a solution (1:2 MeOH/CH$_2$Cl$_2$) in the presence of sodium hydroxide and then the metal salt FeCl$_2$ (0.61 g, 4.8 mmol) was added in 15 mL of distilled water followed by addition 15 mL ethanolic solution of 2-aminopyridine (0.45 g, 4.8 mmol), and the resultant product was refluxed for 4 h and then cooled and filtered. Light-yellow precipitate formed and was collected.

3. Results and Discussion

The nickel(II), copper(II), manganese(II), and iron(II) coordination compounds were prepared by the reaction of 1,3-bis(diphenylphosphino)propane with metal salts and 2-aminopyridine. The prepared four compounds were found to react in the molar ratio 1:1: 1 metal: DPPP: APY. In addition, these compounds are air stable and insoluble in
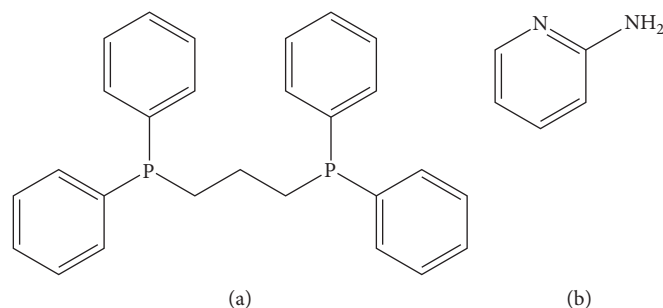
Figure 1: Structure of the ligands. (a) 1,3-Bis(diphenylphosphino)propane. (b) 2-Aminopyridine.

common organic solvents but sparingly soluble in dimethylsulphoxide. The conductivities of the compounds were measured in DMSO using 10^{-3} M solutions of the complexes. The molar conductivity values of the transition metal compounds were 59, 40, 32, and 52 Λm Scm^2 mol^{-1}), respectively. The compositions of the complexes supported by the elemental analysis are recorded together with color in Table 1.

3.1. FT-IR Spectra.
The main infrared spectra of these compounds are listed in Table 2. A comparison of the FT-IR spectra of the complexes 1, 2, 3, and 4 with those of the free DPPP and APY ligands reveals interesting features relating to the metal-ligand (M-L) interactions. From the FT-IR spectra, it is found that the P-PH band, which shows at 1440 cm^{-1} in the spectrum of DPPP, is shifted to a lower wave number (1430–1434 cm^{-1}), indicating a sharing of this group in the bonding with the metal ions [24]. The stretching frequencies of $\nu(NH_2)$ are observed at 3440 cm^{-1} in all complexes; the spectrum almost undergoes no shift, indicating the nonparticipation of this group in the coordination [25]. On the other hand, the stretching vibration of pyridine group located at 1617 (ν) $C = C$ and 1473 (ν) $C = N$ cm^{-1} in the APY ligand exhibits a notable shift to a wave number (1608–1624) and (1478–1482 cm^{-1}) in all complexes, respectively [25]. The C-N stretching in the ring bands of the APY ligand are shifted to lower wave numbers in the range of 1024–1030 cm^{-1} [25]. In the IR spectrum of the free APY, $\nu(C-NH_2)$ occurs at 1140 cm^{-1} with no shift in the spectra of the complexes [26]. These results confirm that the pyridine groups are coordinated to the metal ions as a monodentate through the N-atom. The very strong band for the P-C vibration of free forms of phosphine ligand displays a shift from 690 cm^{-1} to a lower wave number (681–694 cm^{-1}) [27]. The bands between 2850–2923 and 3020–3046 cm^{-1} are due to the absorption of the phenyl and CH_2 groups [27]. From these discussions, it is concluded that DPPP coordinates to the metal ions in a bidentate mode through phosphorus atoms. A broad diffused band with medium intensity located in the range 3488–3496 cm^{-1} may be assigned to $\nu(OH)$ in the lattice H_2O in (1) and (4) complexes [28]. For the complexes 1–4, the νOH stretching vibration of coordinated H_2O appears at the 3315–3360 cm^{-1} region [29]. The IR spectra of the complexes 1–4 appear as a band at 734–739 cm^{-1} assigned to $\rho(H_2O)$, which indicates the

presence of coordinated water [18]. Metal-oxygen, M-nitrogen, and M-phosphorus vibration bands appear at 504–510, 470–482, and 432–448 cm^{-1} district, respectively (Figure 2) [30, 31].

3.2. Electronic Spectra.
The UV-Visible spectra of the complexes have been registered in dimethylsulphoxide. The results are manifested in Table 3. The spectra show two distinct bands in the ranges 36,764–39,840 cm^{-1} and 29,325–32,573 cm^{-1}, which attributed to $\pi \longrightarrow \pi*$ and $n \longrightarrow \pi*$ transitions within DPPP and APY moieties, respectively [27, 32, 33]. On the other hand, in the visible region of spectra, there are characteristic bands attributed to d-d transitions for Ni(II), Cu(II), Mn(II), and Fe(II). For Ni(II), the band is located at the 19,920 cm^{-1} region which is assigned to d-d transition. This band is typical for the octahedral Ni(II) complexes. In the visible spectra of Cu(II), Mn(II), and Fe(II) complexes, the d-d bands are observed in 20,161, 20,040, and 19,841 cm^{-1}, respectively, as expected for octahedral Cu(II), Mn(II), and Fe(II).

3.3. Magnetic Moments.
The magnetic moments of the complexes were measured. The Ni(II) complex has a magnetic moment located in the range 3.20 BM. As foretelled for a high spin d^8 system with two unpaired electrons which falls in the range expected for octahedral Ni(II) compounds [34]. Copper(II) complex gave a value of magnetic moment 1.74 BM [34]. The magnetic moment of the iron complex (5.46 BM) measured at room temperature suggests a high spin d^6 configuration of octahedrally coordinated Fe^{2+} ions [35]. In the case of Mn(II) a compound the value of the magnetic moment 5.30 BM typical for high spin d^5 system with five unpaired electrons with octahedral arrangement around Mn(II) [34, 36]. From the foregoing data, the structure of the compounds can be postulated as follows (Figures 3 and 4).

3.4. Thermal Analysis Studies.
Regarding [Ni(DPPP)(APY)(H_2O)Cl_2].H_2O complex, its decomposition proceeds in five steps (Figure 5). The first and second correspond to the loss of one crystalline H_2O and one coordinated H_2O molecule (calc. 5.36%, found 4.92%) (DTG peak at 72, 122°C), for which a broad, endothermic peak appears in the DTA curve at 74 and 124°C. The third and fourth mass loss is

TABLE 1: Color, elemental analysis, and decomposition point of the mixed ligand complexes.

Complex	MF MW	Color	Found (Calcd.%)		
			C	H	N
[Ni(DPPP)(APY)(H$_2$O)Cl$_2$].H$_2$O 1	C$_{32}$H$_{36}$N$_2$NiP$_2$O$_2$Cl$_2$ 672.2	Pale brown	58.42 (57.17)	6.02 (5.39)	4.36 (4.16)
[Cu(DPPP)(APY)(H$_2$O)Cl$_2$] 2	C$_{32}$H$_{34}$N$_2$CuP$_2$OCl$_2$ 659.02	Light green	58.68 (58.31)	5.72 (5.19)	4.52 (4.24)
[Mn(DPPP)(APY)(H$_2$O)Cl$_2$] 3	C$_{32}$H$_{34}$N$_2$MnP$_2$OCl$_2$ 650.41	Dark brown	60.65 (59.08)	5.84 (5.26)	4.78 (4.30)
[Fe(DPPP)(APY)(H$_2$O)Cl$_2$].2H$_2$O 4	C$_{32}$H$_{38}$N$_2$FeP$_2$O$_3$Cl$_2$ 687.38	Light yellow	56.28 (55.91)	6.05 (5.57)	4.35 (4.07)

TABLE 2: The infrared spectral data (cm^{-1}) of the ligand and their complexes.

Assignment	DPPP	APY	Ni(II) complex	Cu(II) complex	Mn(II) complex	Fe(II) complex
vO-H$_{lattice\ water}$	—	—	3488-	—	—	3496-
vO-H$_{coordinated\ water}$			3320	3315	3338	3360
vC=C	—	1617	1615	1624	1622	1608
vC=N	—	1473	1479	1482	1478	1480
P-PH	1440	—	1434	1433	1430	1430
vC-N$_{in\ ring}$	—	1028	1026	1030	1024	1027
ρOH$_2$	—	—	738	739	734	736
P-C	690	—	694	691	687	681
M-O	—	—	510	504	505	507
M-N	—	—	482	470	474	476
M-P	—	—	448	440	432	434

v: stretching and ρ: rocking.
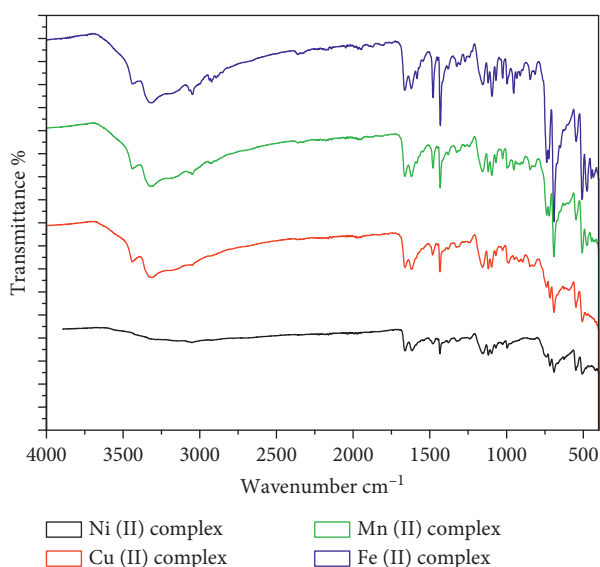
FIGURE 2: FT-IR spectra of Ni(II), Cu(II), Mn(II), and Fe(II) complexes.

Legend:
- Ni (II) complex
- Cu (II) complex
- Mn (II) complex
- Fe (II) complex

TABLE 3: Electronic spectral data of free ligand and its complexes.

Ligands and complexes	v_{max} (cm^{-1})	Assignment	$\mu_{eff.}$ (BM)
DPPP	40,000	$\pi \longrightarrow \pi^*$	—
APY	31,746	$n \longrightarrow \pi^*$	—
	19,920	d-d transition	
Ni(II) complex	31,948	$n \longrightarrow \pi^*$	3.20
	36,764	$\pi \longrightarrow \pi^*$	
	20,161	d-d transition	
Cu(II) complex	29,325	$n \longrightarrow \pi^*$	1.74
	39,840	$\pi \longrightarrow \pi^*$	
	20,040	d-d transition	
Mn(II) complex	32,573	$n \longrightarrow \pi^*$	5.30
	36,900	$\pi \longrightarrow \pi^*$	
	19,841	d-d transition	
Fe(II) complex	31,847	$n \longrightarrow \pi^*$	5.46
	37,037	$\pi \longrightarrow \pi^*$	

concerned to the expulsion of the 2-aminopyridine ligand and chlorine (calc. 24.54%, found 23.69%) (DTG peak at 312, 373°C). This step is marked on the DTA curve by an exothermic effect at 314 and 375°C. The subsequent steps are the decomposition products of the remainder and the rest of the organic ligand. The residue is assigned to be NiO as indicated by the mass loss (calc. 11.10%, found 10.24%) (Scheme 1).

Regarding [Cu(DPPP)(APY)(H$_2$O)Cl$_2$] complex, the TG, DTG, and DTA curves of this compound show that the thermal decomposition processes involve four stages. The first stage occurs in the temperature range 58–145°C due to the release of the H$_2$O molecules (calc. 2.73%, found 2.52%). At this step, a DTG peak appears at 70°C and a broad endothermic effect is recorded in the DTA trace at 73°C. The second step represents a detachment of APY ligand as indicated by mass loss consideration (calc. 14.27%, found 14.05%). This step is manifested in the DTG curve as a peak at 258°C and the DTA trace furnishes an exothermic effect at 260°C. The decomposition of the rest complex proceeds in
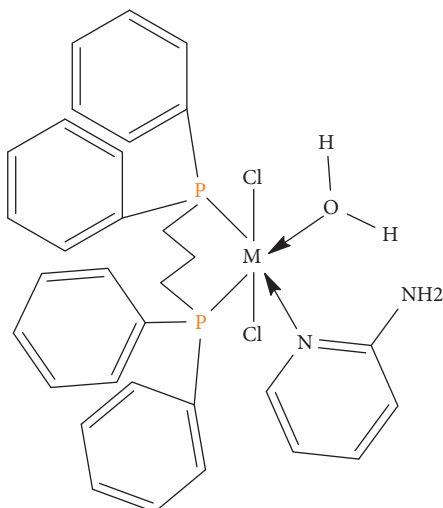
FIGURE 3: Structure of complexes $[M(DPPP)(APY)(H_2O)Cl_2].xH_2O$, where M = Ni(II), Cu(II), Mn(II) or Fe(II) and x = 0, 1, or 2 molecules of H_2O.
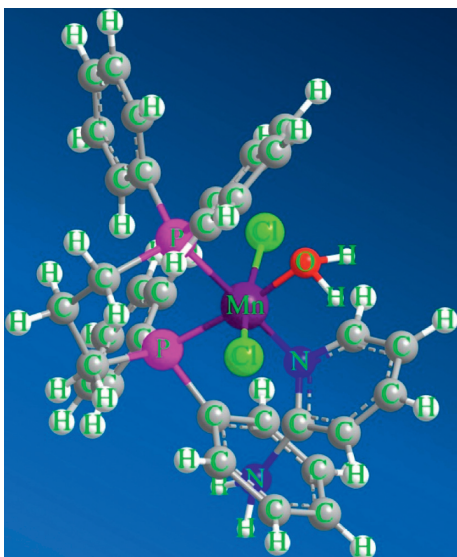

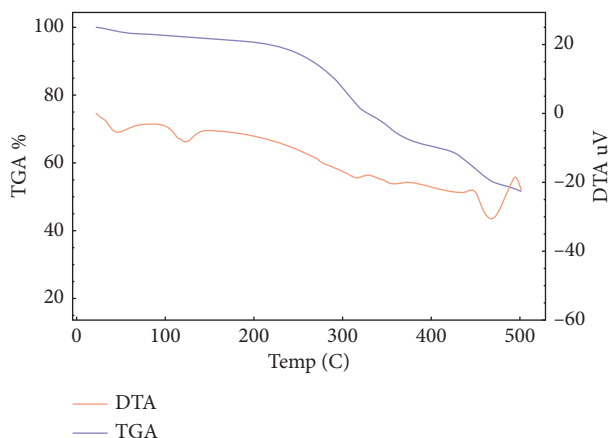FIGURE 4: A perspective view of the complete coordination around Mn(II) complex.

FIGURE 5: TGA and DTA thermograms of Ni(II) complex.

the next step leaving a stable residue of CuO (calc. 12.06%, found 11.56%).

Regarding $[Mn(DPPP)(APY)(H_2O)Cl_2]$ complex, the compound undergoes a stepwise decomposition in three distinct steps of mass loss, namely, at 54–106, 107–320, and 322–600°C. The first step is consistent with the release of H_2O molecules (calc. 2.77%, found 2.45%). It has a DTG peak at 80°C corresponding to an endothermic peak at 82°C in the DTA trace. In the 2nd step, elimination of the (APY) ligand occurs (calc. 14.46%, found 13.98%). A DTG peak at 296°C with a corresponding broad exothermic peak at 298°C in the DTA trace is observed. The third step represents the thermal decomposition of the rest of the complex. The final product of the compound is compatible with MnO (calc. 10.90%, found 9.97%).
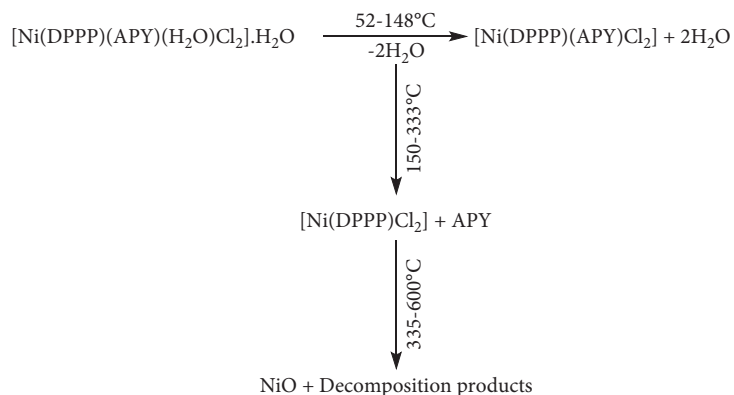
Regarding $[Fe(DPPP)(APY)(H_2O)Cl_2].2H_2O$ complex, the thermogram of $[Fe(DPPP)(APY)(H_2O)Cl_2].2H_2O$ consists of four decomposition stages, namely, at 57–165, 167–278, 280–402, and 404–600°C. The 1st mass loss correlates well with the corresponding of three water molecules, namely, two crystalline and one coordinated, and this may be attributed to an ion-dipole interaction between iron and water (calc. 7.86%, found 7.27%). This step (DTG peak at 81°C) is characterized by an endothermic peak in the DTA curve at 83°C. The second, third, and fourth steps correspond to the decomposition products of the remaining ligands. The final product is assigned to be FeO as indicated by the mass loss in the TG curve (calc. 10.44%, found 10.32%).

3.5. *Kinetic Studies.* Nonisothermal kinetic study of the four coordination compounds was carried out applying the Coats–Redfern and Horowitz–Metzger methods (Figures 6–8). The kinetic parameters for all complexes are calculated for the first, second, and third steps according to the Coats–Redfern method and are cited in Tables 4 and 5.

3.6. *Decomposition Rate and Stability of the Complexes.* The decomposition rates of the four complexes have concluded the plotting of the fraction decomposition (α) against the temperature (T) of the decomposition for the first stage as shown in (Figure 8)

The stabilities of the Ni(II), Cu(II), Mn(II), and Fe(II) coordination complexes could be correlated. In addition to that, the following are the stability orders of the four complexes and the decomposition rates are based on the following:

   (i) The stability order at the initial temperature of the 1st stage of the anhydrous complexes

   (ii) The temperature of the inflection point

   (iii) DTG maximum temperatures (decomposition rate) and initial temperatures (sequence of stability) that are in parentheses

   (iv) The regression of the curves (α against T) indicates that the complexes decompose by various decomposition rates based on the respective metal ions

$$[Ni(DPPP)(APY)(H_2O)Cl_2] \cdot H_2O \xrightarrow[-2H_2O]{52\text{-}148°C} [Ni(DPPP)(APY)Cl_2] + 2H_2O$$

$$\downarrow 150\text{-}333°C$$

$$[Ni(DPPP)Cl_2] + APY$$

$$\downarrow 335\text{-}600°C$$

$$NiO + \text{Decomposition products}$$

SCHEME 1: The decomposition stages for nickel(II) complex in dynamic air.
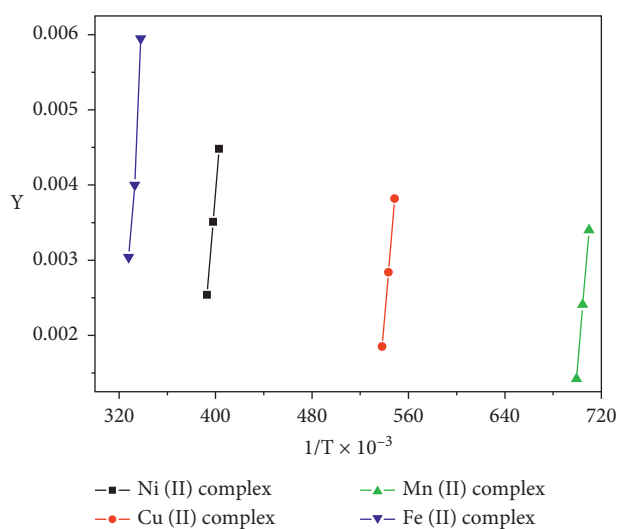
FIGURE 6: Coats–Redfern plot for the complex 2nd step in dynamic air.
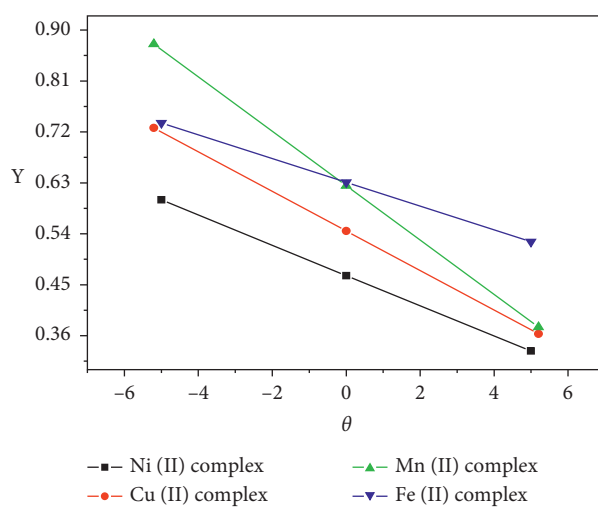
FIGURE 7: Horowitz–Metzger plot for complex 2nd step in dynamic air.

(−Ve) ΔS^* values for the different steps of decomposition of nickel(II), copper(II), manganese(II), and iron(II) compounds propose that the activated complexes are in higher order than the reactants and also that the reactions are slower than the normal level. The different numbers of enthalpies (ΔH^*) and free energy (ΔG^*) of the four
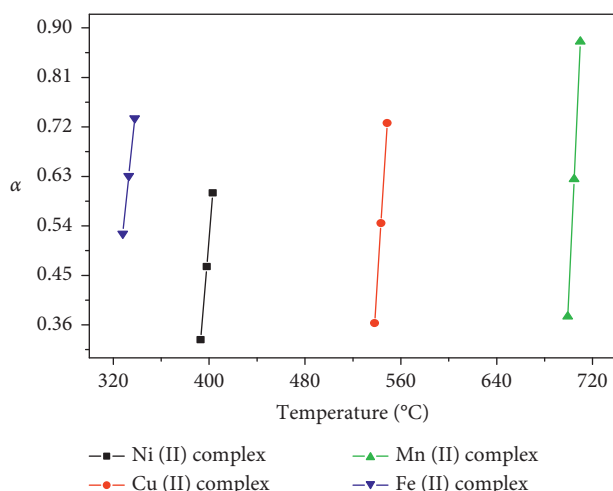
FIGURE 8: Fraction decomposed (α) and temperature plots (T) of the complexes.

TABLE 4: Kinetic parameters for the thermal decomposition of Ni(II) and Cu(II) complexes using nonmechanistic equations in dynamic air by Coats–Redfern equation.

Step								
			$[Ni(DPPP)(APY)(H_2O)Cl_2].H_2O$				$[Cu(DPPP)(APY)(H_2O)Cl_2]$	
	n	r	E kJ mol^{-1}	Z s^{-1}	n	r	E kJ mol^{-1}	Z s^{-1}
1st	0.00	0.9968	36.70	7.24×10^2	0.00	0.9992	39.15	7.76×10^2
	0.33	0.9946	49.63	10.00×10^2	0.33	0.9999	46.71	9.33×10^2
	0.50	**1.0000**	57.62	11.48×10^2	0.50	**1.0000**	51.17	10.23×10^2
	0.66	0.9998	65.80	13.18×10^2	0.66	0.9999	55.46	11.22×10^2
	1.00	0.9981	86.53	17.37×10^2	1.00	0.9993	65.57	13.18×10^2
	2.00	0.9893	169.64	35.48×10^2	2.00	0.9958	102.21	20.89×10^2
2nd	0.00	0.9961	74.17	14.79×10^2	0.00	0.9574	17.07	3.46×10^2
	0.33	0.9972	83.68	16.59×10^2	0.33	0.9647	19.99	3.98×10^2
	0.50	0.9980	89.07	17.78×10^2	0.50	0.9673	21.54	4.26×10^2
	0.66	0.9984	94.14	19.05×10^2	0.66	0.9703	23.22	4.57×10^2
	1.00	0.9989	105.55	21.37×10^2	1.00	0.9753	26.91	5.42×10^2
	2.00	**1.0000**	144.22	29.51×10^2	2.00	**0.9859**	40.09	7.94×10^2
3rd	0.00	**0.9994**	29.22	5.75×10^2	0.00	0.9978	17.40	3.46×10^2
	0.33	0.9969	34.03	6.76×10^2	0.33	0.9992	21.49	4.26×10^2
	0.50	0.9951	36.76	7.24×10^2	0.50	0.9997	23.86	4.78×10^2
	0.66	0.9929	39.59	7.94×10^2	0.66	0.9999	26.15	5.24×10^2
	1.00	0.9873	46.12	9.12×10^2	1.00	**1.0000**	31.76	6.30×10^2
	2.00	0.9678	70.27	14.12×10^2	2.00	0.9983	52.30	10.47×10^2

Bold values of r represent the best fit values of n, E, and Z.

TABLE 5: Kinetic parameters for the thermal decomposition of Mn(II) and Fe(II) complexes using nonmechanistic equations in dynamic air by Coats–Redfern equation.

Step								
			$[Mn(DPPP)(APY)(H_2O)Cl_2]$				$[Fe(DPPP)(APY)(H_2O)Cl2].2H_2O$	
	n	r	E kJ mol^{-1}	Z s^{-1}	n	r	E kJ mol^{-1}	Z s^{-1}
1st	0.00	**0.9951**	14.92	3.01×10^2	0.00	0.9926	25.16	5.01×10^2
	0.33	0.9909	18.16	3.71×10^2	0.33	0.9947	31.48	6.30×10^2
	0.50	0.9886	20.07	3.98×10^2	0.50	0.9961	35.09	6.91×10^2
	0.66	0.9860	21.98	4.36×10^2	0.66	0.9968	38.89	7.76×10^2
	1.00	0.9812	26.57	5.24×10^2	1.00	0.9978	47.34	9.33×10^2
	2.00	0.9664	43.24	8.70×10^2	2.00	**0.9996**	78.89	15.8×10^2
2nd	0.00	0.9926	33.75	6.76×10^2	0.00	**0.9934**	128.37	25.70×10^2
	0.33	0.9970	41.08	8.12×10^2	0.33	0.9920	140.46	28.18×10^2
	0.50	0.9984	45.26	8.91×10^2	0.50	0.9917	146.58	29.51×10^2
	0.66	0.9994	49.73	10×10^2	0.66	0.9913	152.69	30.90×10^2
	1.00	**1.0000**	60.19	12.02×10^2	1.00	0.9904	166.68	33.88×10^2
	2.00	0.9952	100.23	19.95×10^2	2.00	0.9870	210.84	41.68×10^2

Bold values of r represent the best fit values of n, E, and Z.

TABLE 6: Thermodynamic parameters for the thermal decomposition of the compounds.

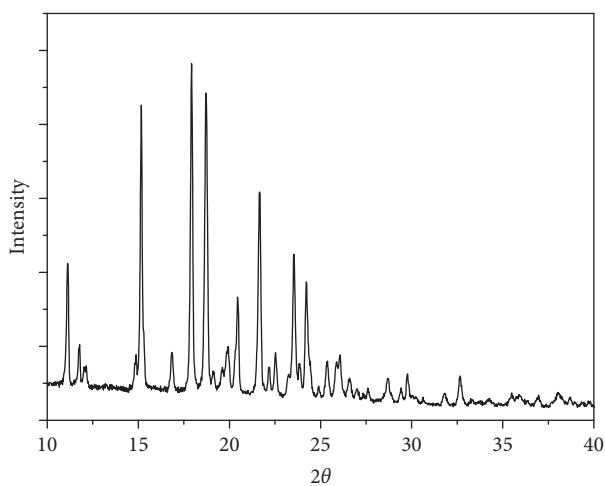| Complex	Step	ΔS^* kJ mol^{-1}K^{-1}	ΔH^* kJ mol^{-1}	ΔG^* kJ mol^{-1}
Ni(II) complex	1st	−190.92	33.98	96.41
		−188.23	46.91	108.46
		−187.09	54.90	116.07
		−185.94	63.08	123.88
		−183.64	83.81	143.86
		−177.70	166.92	225.02
Cu(II) complex	1st	−190.10	36.50	96.91
		−188.57	44.06	103.98
		−187.81	48.52	108.20
		−187.04	52.81	112.25
		−185.70	62.92	121.93
		−181.87	99.56	157.35
Mn(II) complex	1st	−203.52	9.77	135.66
		−201.78	13.01	137.83
		−201.19	14.92	139.37
		−200.43	16.83	140.81
		−198.91	21.42	144.46
		−194.69	38.09	158.52
Fe(II) complex	1st	−194.13	22.39	87.03
		−192.23	28.71	92.72
		−191.46	32.32	96.07
		−190.49	36.12	99.55
		−188.96	44.57	107.49
		−184.56	76.12	137.57

FIGURE 9: XRD of nickel(II) complex.
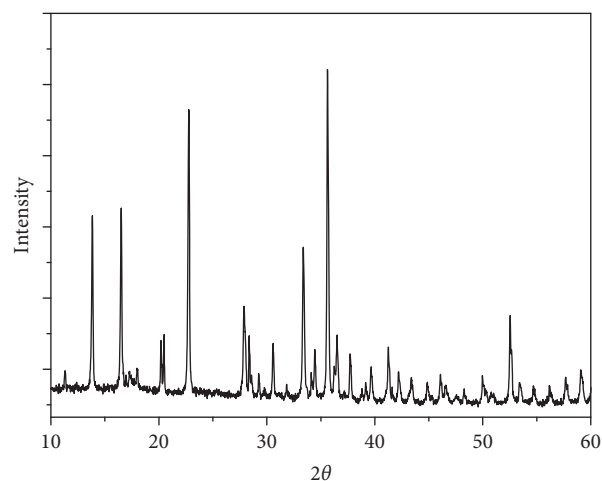
FIGURE 10: XRD of copper(II) complex.

compounds turn on the effect of the structure, each of the metal ions on the thermal stability of the coordination compounds. The (a +Ve) values of ΔG^* indicated that during the decomposition, reaction is not spontaneous (Table 6).

3.7. X-Ray Powder Diffraction of the Four Complexes. The X-ray powder diffraction types were recorded for the complexes 1–4. The diffraction shapes indicate that the four compounds are crystalline (Figures 9–12). The crystal data for nickel(II), copper(II), Mn(II), and Fe(II) mixed-ligand

coordination complexes belong to the monoclinic, triclinic, and monoclinic crystal system, analyzed by Scherrer's equation. The crystal data for all compounds are listed in Table 7.

3.8. Biological Activity of the Coordination Compounds. Prepared compounds of nickel(II), copper(II), manganese(II), and iron(II) were tested for *in vitro* antimicrobial activity and evaluated against selected bacterial and fungal strains (Figures 13–18). Three strains of gram-positive cocci (*Staphylococcus epidermidis, Enterococcus faecalis,*
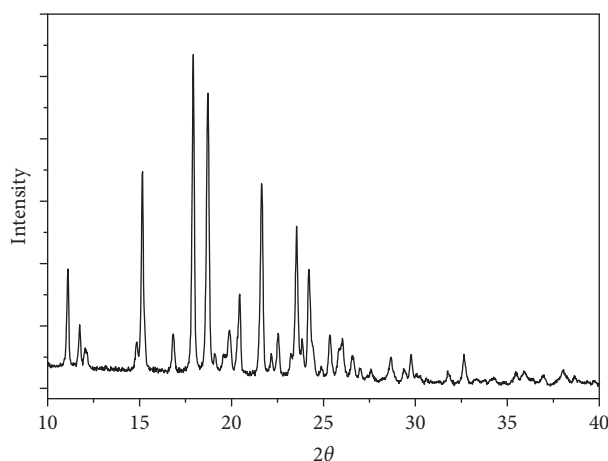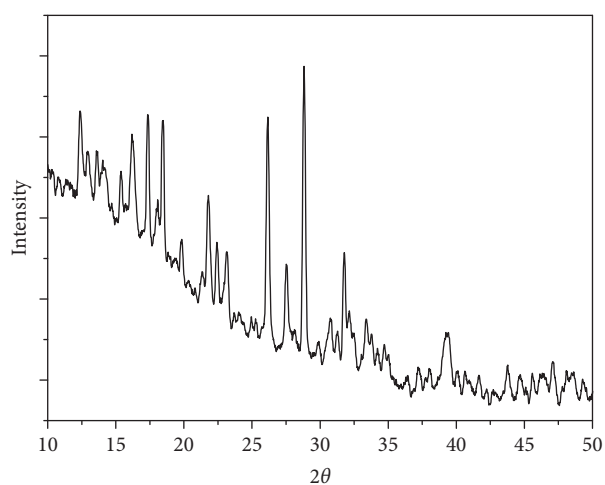
Figure 11: XRD of manganese(II) complex.

Figure 12: XRD of iron(II) complex.

Table 7: X-ray powder diffraction crystal data of complexes.

Parameters	Ni(II) complex	Cu(II) complex	Mn(II) complex	Fe(II) complex
Empirical formula	$C_{32}H_{36}N_2NiP_2O_2Cl_2$	$C_{32}H_{34}N_2CuP_2OCl_2$	$C_{32}H_{34}N_2MnP_2OCl_2$	$C_{32}H_{38}N_2FeP_2O_3Cl_2$
Formula weight	672.2	659.02	650.41	687.38
Crystal system	Triclinic	Monoclinic	Triclinic	Monoclinic
a (Å)	15.509	13.140	15.503	11.491
b (Å)	16.785	9.857	16.788	7.393
c (Å)	10.223	6.018	10.224	9.781
Alfa (°)	103.303	90.00	103.295	90.00
Beta (°)	96.349	103.20	96.342	117.25
gamma (°)	105.685	90.00	105.656	90.00
Volume of unit cell (Å3)	2450.6	758.99	2450.9	738.7

and *Staphylococcus aureus*), two strains of gram-negative Bacilli (*Pseudomonas aeruginosa* and *Escherichia coli*), one stain of yeast like fungi (*Candida albicans*), and 2 molds (*Aspergillus fumigatus* and *Aspergillus flavus*) were used. The data showed that all complexes have good activity against bacterial strains. Yeast-like fungal stain and mold strains showed good activity mainly toward Ni(II), Cd(II), and Co(II) complexes. Gram-positive bacteria were found to be more sensitive to all tested extracts with significantly higher zones of inhibition than those of gram-negative bacteria and fungal strains. Nickel(II), cadmium(II), and cobalt(II) complexes show higher inhibition zone than the
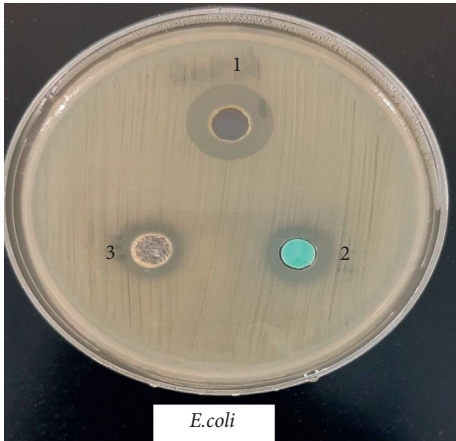
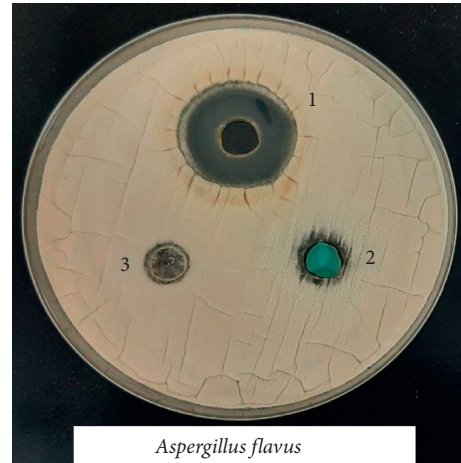Figure 13: Microbiological screening of Ni(II), Cu(II) and Mn(II) complexes against *E.coli.*
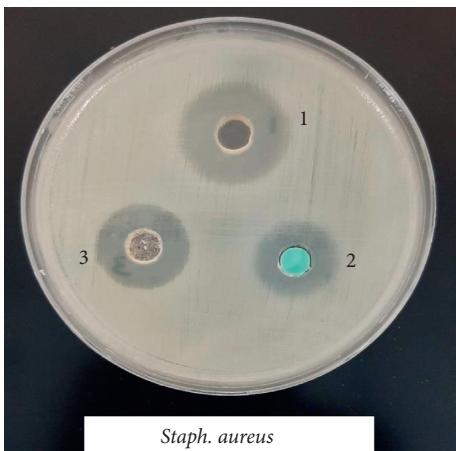

Figure 14: Microbiological screening of Ni(II), Cu(II) and Mn(II) complexes with *S. aureus.*

Figure 15: Microbiological screening of Ni(II), Cu(II) and Mn(II) complexes with *S. epidermidis.*

Figure 16: Microbiological screening of Ni(II), Cu(II) and Mn(II) complexes against *Aspergillus flavus.*
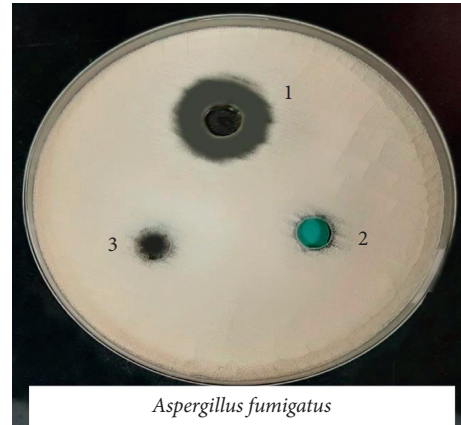

Figure 17: Microbiological screening of Ni(II), Cu(II) and Mn(II) complexes against *Aspergillus fumigatus.*
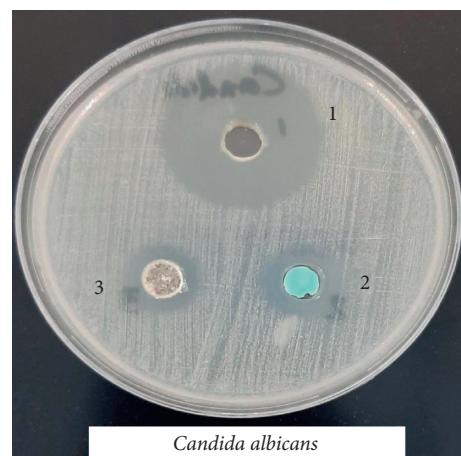

Figure 18: Microbiological screening of Ni(II), Cu(II) and Mn(II) complexes against *Candida albicans.*

TABLE 8: Microbiological screening of the complexes.

Tested organisms	Ni(II)	Cu(II)	Mn(II)	Fe(II)
Staphylococcus aureus	24	17	21	16
Staphylococcus epidermidis	23	11	22	15
Enterococcus faecalis	24	13	20	15
Escherichia coli	18	14	14	13
Pseudomonas aeruginosa	16	13	11	13
Candida albicans	35	15	15	16
Aspergillus fumigatus	19	—	—	—
Aspergillus flavus	17	—	—	—
Erythromycin (E15)*	24 mm			
Ketoconazole (KET 50)**	25 mm			

*Control of antibacterial; **control of antifungus.

other tested extract complexes as stated in Table 8. The zone of inhibition around the wells is measured in millimeters (mm) by a ruler.

4. Conclusion

A number of new one-dimensional nickel(II), copper(II), manganese(II), and iron(II) metal supramolecular coordination compounds of 1,3-bis(diphenylphosphino)propane and 2-aminopyridine have been prepared and characterized by various spectral and physical techniques. From the X-ray analysis, different crystal systems, monoclinic, triclinic, and orthorhombic system for the complexes, were found. The results of antimicrobial activity observed good biological activity for the four compounds, but the nickel(II) complex was over the other three complexes.

Data Availability

The data used to support the findings of this study are available from the corresponding author upon request.

Conflicts of Interest

The authors declare that they have no conflicts of interest.

References

[1] Y. Yuan, H.-L. Han, S. Lin et al., "Synthesis, structural characterization, stability, antibacterial activity and spectroscopic properties (THz) of five new polynuclear silver(I) complexes with 1, 10-phenanthroline derivative and 1, 3-bis (diphenylphosphino) propane (dppp)," *Polyhedron*, vol. 119, pp. 184–193, 2016.

[2] T. Veysel, A. Yilmaz, C. Icsel, M. Aygun, M. Erkisa, and E. Ulukay, "Pd(II) and Pt(II) saccharinate complexes of bis (diphenylphosphino) propane/butane: synthesis, structure, antiproliferative activity and mechanism of action," *European Journal of Medicinal Chemistry*, vol. 158, pp. 534–547, 2018.

[3] A. Mannu, G. Vlahopoulou, C. Kubis, H.-J. Drexler, and H.-J. Drexler, "Synthesis and characterization of [Rh(PP)(PP)]X complexes (PP = DPPE or DPPP, X = Cl– or BF4-). phosphine exchange and reactivity in transfer hydrogenation conditions," *Journal of Organometallic Chemistry*, vol. 885, pp. 59–64, 2019.

[4] G. Kalaiarasi, S. Dharani, H. Puschmann, and R. Prabhakaran, "Synthesis, structural characterization, DNA/protein binding and antioxidant activities of binuclear Ni(II) complexes containing ONS chelating ligands bridged by 1, 3-bis (diphenylphosphino) propane," *Inorganic Chemistry Communications*, vol. 97, pp. 34–38, 2018.

[5] M. Theresa, W.-Li Jia, and S. Wang, "Phosphorescent Cu(I) complexes of 2-(2′-pyridylbenzimidazolyl) benzene: impact of phosphine ancillary ligands on electronic and photophysical properties of the Cu(I) complexes," *Inorganic Chemistry*, vol. 45, no. 1, pp. 147–155, 2006.

[6] G. Hu, W. Wei, P. Shuai, G. Lei, and S. Qing, "A series of copper(I) complexes with electron donor/acceptor embedded ligands: synthesis, photophysical and electroluminescent properties," *Journal of Luminescence*, vol. 131, no. 2, pp. 238–243, 2011.

[7] D. G. Cuttell, S.-M. Kuang, P. E. Fanwick, D. R. McMillin, and R. A. Walton, "Simple Cu(I) complexes with unprecedented excited-state lifetimes," *Journal of the American Chemical Society*, vol. 124, no. 1, pp. 6-7, 2002.

[8] P. Coppens, I. I. Vorontsov, T. Graber et al., "Geometry changes of a Cu(I) phenanthroline complex on photoexcitation in a confining medium by time-resolved X-ray diffraction," *Journal of the American Chemical Society*, vol. 126, no. 19, pp. 5980-5981, 2004.

[9] K. Saito, T. Arai, N. Takahashi, T. Tsukuda, and T. Tsubomura, "A series of luminescent Cu(i) mixed-ligand complexes containing 2, 9-dimethyl-1, 10-phenanthroline and simple diphosphine ligands," *Dalton Transactions*, vol. 37, no. 37, pp. 4444–4448, 2006.

[10] C. J. Jones, "Transition metals as structural components in the construction of molecular containers," *Chemical Society Reviews*, vol. 27, no. 4, pp. 289–299, 1998.

[11] M. W. Hosseini, "Molecular tectonics: from simple tectons to complex molecular networks," *Accounts of Chemical Research*, vol. 38, no. 4, pp. 313–323, 2005.

[12] M. J. Rosseinsky, "Recent developments in metal-organic framework chemistry: design, discovery, permanent porosity and flexibility: metal-organic open frameworks," *Microporous and Mesoporous Materials*, vol. 73, no. 1-2, pp. 15–30, 2004.

[13] H. Lee, T. H. Noh, and O.-S. Jung, "Construction of kagome-type networks via tridentate ligand: structural properties as alcohol reservoir," *CrystEngComm*, vol. 15, no. 10, pp. 1832–1835, 2013.

[14] O.-S. Jung, Y. J. Kim, Y.-A. Lee, J. K. Park, and H. K. Chae, "Smart molecular helical springs as tunable receptors," *Journal of the American Chemical Society*, vol. 122, no. 41, pp. 9921–9925, 2000.

[15] G. Kalaiarasi, R. Jain, A. Shanmugapriya, H. Puschman, P. Kalaivani, and R. Prabhakaran, "New binuclear Ni(II) metallates as potent antiproliferative agents against MCF-7 and HeLa cells," *Inorganica Chimica Acta*, vol. 462, pp. 174–187, 2017.

[16] H. Fuhrmann, S. Brenner, P. Arndt, and R. Kempe, "Octahedral group 4 metal complexes that contain amine, amido, and aminopyridinato ligands : synthesis, structure, and application in r-olefin oligo-and polymerization," *Inorganic Chemistry*, vol. 1669, no. 96, pp. 6742–6745, 1996.

[17] C. Yenikaya, N. Büyükkidan, M. Sari et al., "Synthesis, characterization, and biological evaluation of Cu(II) complexes with the proton transfer salt of 2, 6-pyridinedicarboxylic acid and 2-amino-4-methylpyridine," *Journal of Coordination Chemistry*, vol. 64, no. 19, pp. 3353–3365, 2011.

[18] S. Mistri, E. Zangrando, and S. C. Manna, "Cu(II) complexes of pyridine-2, 6-dicarboxylate and N-donor neutral ligands: synthesis, crystal structure, thermal behavior, DFT calculation and effect of aromatic compounds on their fluorescence," *Inorganica Chimica Acta*, vol. 405, pp. 331–338, 2013.

[19] R. K. Poddar and U. Agarwala, "Reactions of Ru(PPh₃)₂Cl₂ and [Ru(AsPh₃)₂Cl₂]₂ with various donor molecules," *Journal of Inorganic and Nuclear Chemistry*, vol. 35, no. 11, pp. 3769–3779, 1973.

[20] M. Y. Jibrin and A. N. Suleiman, "Synthesis and spectroscopic characterization of Ni(II) and Cu(II) schiff base transition metal complexes from a mix of drugs sulfamethaxole with 2-aminopyridine and benzaldehyde," *Journal of Research in Chemistry*, vol. 1, no. 1, pp. 32–35, 2020.

[21] W. X. Ma, B. H. Qian, J. Chen, O. Sha, and X. Y. J. Xu, "Synthesis, crystal structure and spectral characterization of the complex [Zn(CH₃CH₂CH₂CH₂N = CHC₆H₄O)₂]," *Journal of Synthetic Crystals*, vol. 35, no. 6, pp. 1363–1367, 2006.

[22] L. G. Wang, Z. Y. Wang, and S. G. Liu, "Synthesis, characterization and crystal structure of zinc(II) complex with (chlorophenyl) benzimidazole," *Journal of Chemical Research and Application*, vol. 14, no. 3, pp. 313–315, 2002.

[23] Z. M. Wang, Z. F. Zhou, H. K. Lin et al., "Synthesis, characterization of α-(aminomethyl) pyridine derivative of 2, 9-dimethyl-1, 10-phenanthroline and potentiometric determination of the stability constants of its complexes with manganese(II), cobalt(II), nickel(II), copper(II) and zinc(II)," *Inorganic Chemistry*, vol. 16, no. 2, pp. 267–272, 2000.

[24] L. Daasch and D. Smith, "Infrared spectra of phosphorus compounds," *Analytical Chemistry*, vol. 23, no. 6, pp. 853–868, 1951.

[25] S. P. Jose and S. Mohan, "Vibrational spectra and normal coordinate analysis of 2-aminopyridine and 2-amino picoline," *Spectrochimica Acta Part A: Molecular and Biomolecular Spectroscopy*, vol. 64, no. 1, pp. 240–245, 2006.

[26] A. Colette, M. O. Agwara, D. M. Yufanyi, M. A. Conde, R. Jagan, and K. O. Eyong, "Synthesis, crystal structure, and antimicrobial properties of a novel 1-D cobalt coordination polymer with dicyanamide and 2-aminopyridine," *International Journal of Inorganic Chemistry*, vol. 2015, Article ID 106838, 8 pages, 2015.

[27] V. T. Yilmaz, E. Gocmen, C. Icsel, M. Cengiz, S. Y. Susluer, and O. Buyukgungor, "Di- and polynuclear silver(I) saccharinate complexes of tertiary diphosphane ligands: synthesis, structures, in vitro DNA binding, and antibacterial and anticancer properties," *Journal of Biological Inorganic Chemistry*, vol. 19, no. 1, pp. 29–44, 2014.

[28] A. þ Bravo and J. R. Anacona, "Metal complexes of the flavonoid quercetin: antibacterial properties," *Transition Metal Chemistry*, vol. 26, no. 1-2, pp. 20–23, 2001.

[29] T. H. Rakha, "Transition metal chelates derived from potassium nicotinoyldithiocarbazate (KHNDC)," *Synthesis and Reactivity in Inorganic and Metal-Organic Chemistry*, vol. 30, no. 2, pp. 205–224, 2000.

[30] M. S. Al-Fakeh, "Synthesis, thermal stability and kinetic studies of copper(II) and cobalt(II) complexes derived from 4-aminobenzohydrazide and 2-mercaptobenzothiazole," *European Chemical Bulletin*, vol. 9, no. 10–12, pp. 403–409, 2020.

[31] N. H. Buttrus, A. A. Sabah, E. A. Abdalrazaq, and S. M. Mohamed, "Synthesis and characterization of Ni²⁺, Cu²⁺ and Zn²⁺ complexes with benzimidazole-2-thionate, diphosphene and their reaction with iodine," *Asian Journal of Chemistry*, vol. 25, no. 9, pp. 4856–4860, 2013.

[32] P. Aslanidis, P. J. Cox, S. Divanidis, and A. C. Tsipis, "Copper(I) halide complexes with 1,3-propanebis (diphenylphosphine) and heterocyclic thione ligands: crystal and electronic structures (DFT) of [CuCl(PymtH)(Dppp)], [CuBr(PymtH)(Dppp)], and [Cu(μ-I)(Dppp)]2," *Inorganic Chemistry*, vol. 41, no. 25, pp. 3372–3378, 2002.

[33] C. Yenikaya, M. Poyraz, M. Sarı, F. Demirci, H. İlkimen, and O. Büyükgüngör, "Synthesis, characterization and biological evaluation of a novel Cu(II) complex with the mixed ligands 2, 6-pyridinedicarboxylic acid and 2-aminopyridine," *Polyhedron*, vol. 28, no. 16, pp. 3526–3532, 2009.

[34] M. S. Al-fakeh, "Synthesis and characterization of coordination polymers of 1, 3-di (4-pyridyl)-propane and 2-aminobenzothiazole with Mn(II), Co(II), Cu(II) and Ni(II) ions," *Journal of Chemical and Pharmaceutical Research*, vol. 10, no. 2, pp. 77–83, 2018.

[35] S. Petricek and A. Demsar, "Syntheses and crystal structures of vanadium and iron chloride complexes with diglyme," *Acta Chimica Slovenica*, vol. 62, no. 2, pp. 354–361, 2015.

[36] A. Z. El-Sonbati, M. A. Diab, S. M. Morgan, M. I. Abou-Dobara, and A. A. El-Ghettany, "Synthesis, characterization, theoretical and molecular docking studies of mixed-ligand complexes of Cu(II), Ni(II), Co(II), Mn(II), Cr(III), UO₂(II) and Cd(II)," *Journal of Molecular Structure*, vol. 1200, Article ID 127065, 2020.